# Raman spectroscopic studies of dimyristoylphosphatidic acid and its interactions with ferricytochrome c in cationic binary and ternary lipid-protein complexes

James S. Vincent* and Ira W. Levin‡

*Chemistry Department, University of Maryland Baltimore County, Catonsville, Maryland 21228; and ‡Laboratory of Chemical Physics, National Institute of Diabetes and Digestive and Kidney Diseases, National Institutes of Health, Bethesda, Maryland 20892 USA

ABSTRACT The vibrational Raman spectra of both pure 1-α-dimyristoylphosphatidic acid (DMPA) liposomes and DMPA multilayers reconstituted with ferricytochrome c at pH 7 and pH 4, with either sodium or calcium as the cation, are reported as a function of temperature. Multilayers composed of a 1:1 mol ratio DMPA and dimyristoylphosphatidylcholine with perdeuterated acyl chains (DMPC-$d_{54}$) have also been reconstituted with $\sim 10^{-4}$ M ferricytochrome c for Raman spectroscopic observation. Total integrated band intensities and relative peak height intensity ratios, two spectral Raman scattering parameters used to characterize bilayer properties, are sensitive to the presence of both ferricytochrome c and the cation in the reconstituted liposomes. Temperature profiles, derived from the various Raman intensity parameters for the 3,100–2,800 $cm^{-1}$ lipid acyl chain C-H stretching mode region specifically reflect bilayer perturbations due to the interactions of ferricytochrome c. At pH 4 the calcium DMPA multilamellar gel to liquid crystalline phase transition temperatures $T_m$, defined by either the C-H stretching mode $I_{2850}/I_{2880}$ and $I_{2935}/I_{2880}$ peak height intensity ratios, are 58.5 ± 0.5°C and 60.0 ± 0.3°C, respectively. This difference in $T_m$'s resolves the phase transition process into first an expansion of the lipid lattice and then a melting of the lipid acyl chains. At pH 7 the calcium DMPA liposomes show no distinct phase transition characteristics below 75°C. For sodium DMPA liposomes reconstituted with ferricytochrome c at either pH 4.0 or pH 7.0, spontaneous Raman spectra show altered lipid structures at temperatures above 40°C. Resonance Raman spectra indicate that ferricytochrome c reconstituted in either calcium or sodium DMPA liposomes changes irreversibly above $T_m$. For either the binary lipid or ternary lipid-protein systems reconstituted with DMPC-$d_{54}$, linewidth parameters of the DMPC-$d_{54}$ acyl chain $CD_2$ symmetric stretching modes at 2,103 $cm^{-1}$ provide a sensitive measure of the conformational and dynamic properties of the perdeuterated lipid component, while the 3,000 $cm^{-1}$ C-H spectral region reflects the bilayer characteristics of the DMPA species in the complex. Although calcium clearly induces a lateral phase separation in the DMPA/DMPC-$d_{54}$ system at pH 7.5 (Kouaouci, R., J. R. Silvius, I. Graham, and M. Pezolet. 1985. *Biochemistry.* 24:7132–7140), no distinct lateral segregation of the lipid components is observed in the mixed DMPA/DMPC-$d_{54}$ lipid system in the presence of either ferricytochrome c or the sodium and calcium cations at pH 4.0. However, domain formation, consisting of regions rich in DMPA and DMPC-$d_{54}$, respectively, is suggested for the calcium binary lipid mixture at pH 4.0 by the different values for $T_m$ and $\Delta T$ characterizing the DMPA and DMPC-$d_{54}$ species. Spectral evidence strongly suggests that ferricytochrome c also induces domain formation in the ternary lipid-protein mixtures at pH 7.0, but only for the sodium cation.

## INTRODUCTION

Although phosphatidic acid is only a minor component in the plasma membrane, this negatively charged lipid is a key intermediate in phospholipid biosynthesis (1) and one of the intermediates in the recycling phase of agonist-dependent phosphoinositide metabolism (2). In addition, phosphatidic acid plays a role in calcium transport across membrane (3). In perhaps related phenomena, the interaction of this negatively charged system with calcium cations leads to lateral phase separations in mixed lipid systems (4). Ferricytochrome *c*, the water soluble heme protein involved with mitochondrial electron transport (5), forms complexes with cardiolipin and phosphatidic acid, two of the anionic lipids found in the inner mitochondrial membrane (6). The association of ferricytochrome *c* with phosphatidic acid has been studied by a variety of experimental techniques, including monolayer pressure perturbations (7), electrochemistry (8), and electron paramagnetic resonance (EPR) (9, 10). Spontaneous Raman, resonance Raman, and EPR spectroscopic studies have also focused on the association of ferricytochrome *c* and cardiolipin (11, 12). These studies provide evidence that the protein/lipid interaction affects both the intra- and intermolecular order of the acyl chains in the interior of the lipid bilayer, suggesting considerable protein penetration into the membrane. Ferricytochrome *c*'s side chain penetration into the interface region of the bilayer ostensibly occurs in addition to a bilayer surface electrostatic interaction between the lipid's negative head group charge and the large protein dipole moment arising primarily from the collection of lysine residues surrounding the protein's heme cleft (13). Surprisingly, even the weak electrostatic interaction of ferricytochrome *c* with a zwitterionic lipid, dipalmitoylphos-


0006-3495/91/05/1007/15 $2.00

phatidylcholine, leads to demonstrable acyl chain perturbations within the bilayer (14).

The nature of cation interactions with acidic phospholipids strongly influences the macroscopic and thermotropic properties of a lipid bilayer. Crystallographic investigations of dimyristoylphosphatidic acid (15), showing extensive hydrogen bounding of water between headgroups of neighboring molecules, suggest that the competing effects of pH and cation interaction can alter the nature of hydrogen bonding at the membrane surface. The cation complexes of calcium with phosphatidic acid lipids, for example, are quite stable and form cochleate lipid structures, suggesting spirally folded shells (16). At physiological pH, calcium dimyristoyl- and calcium dipalmitoylphosphatidic acid species show no well defined gel to liquid crystalline phase transition (4, 17) behavior, which is in sharp contrast to that of the calcium complex at acidic pH (pH 4) or that of the sodium and potassium salts of phosphatidic acid at pH 4 or 7, all of which exhibit multilamellar structures and distinct gel to liquid crystalline phase transitions (16–20). The introduction of calcium ions in binary lipid systems, composed of dimyristoylphosphatidic acid and dimyristoylphosphatidylcholine, leads to lateral separation of the lipid components at pH 7.5 (4).

Vibrational Raman spectroscopy represents a sensitive, noninvasive technique for studying the thermotropic behavior of lipid membrane systems (21–26). This spectroscopic approach is particularly suited for studying binary lipid systems as aqueous dispersions in which one component possesses perdeuterated acyl chains (27–29). That is, with the acyl chain methylene carbon-deuterium (C-D) vibrational modes occurring in spectral regions displaced from the acyl chain C-H vibrations, both lipid species can be monitored independently. Spectral peak height intensity ratios and linewidths are used to determine various order/disorder parameters which are characteristic of bilayer assemblies (21, 22, 25). The C-H vibrational peak height intensity parameter, $I_{2850}/I_{2880}$, where the 2,850 and 2,880 $cm^{-1}$ modes refer to the chain methylene $CH_2$ symmetric and asymmetric vibrations, respectively, reflects lateral chain-chain interactions within the bilayer. Disorder/order measures arising from interchain interactions, but with contributions from intrachain trans/gauche isomerizations, are determined from the $I_{2935}/I_{2880}$ intensity parameter, where the 2,935 $cm^{-1}$ feature contains spectral components from Fermi resonance interactions involving the chain methylene moieties and, separately, the C-H symmetric stretching modes of the chain methyl termini of the bilayer lipids (25). Other measures of lateral interchain interaction are determined from linewidth parameters of the 2,103 $cm^{-1}$ perdeuterated acyl chain symmetric methylene C-D stretching modes; namely, $\Delta\nu_{7/8}$, the linewidth at 7/8 of the peak intensity (30). The halfwidth parameter ($\Delta\nu_{1/2}$) for the 2,103 $cm^{-1}$ band reflects intrachain trans/gauche isomerization disorder and increases with the number of gauche conformers induced along the lipid hydrocarbon moiety (30, 31).

In view of the aggregative properties of phosphatidic acid lipids and ferricytochrome *c* and their relevance to the structure and function of the inner mitochondrial membrane, we investigate in the present study by Raman spectroscopy the specific interactions of ferricytochrome *c* first with dimyristoylphosphatidic acid (DMPA) multilayers and then with a mixed bilayer system composed of DMPA and dimyristoylphosphatidylcholine, with perdeuterated acyl chains (DMPC-$d_{54}$), in the presence of either sodium or calcium ions at various pH values. The thermotropic behavior of the cation complexes of pure DMPA and a 1:1 mixture of DMPA and DMPC-$d_{54}$ is also presented as a basis for comparing the protein interactions with the sodium and calcium complexes of both lipid systems. Ferricytochrome *c* interactions are assessed by changes in the gel and liquid crystalline phase Raman spectral order/disorder parameters and by perturbations to the phase transition temperature $T_m$.

## MATERIALS AND METHODS

The sodium salt of 1-α-dimyristoylphosphatidic acid (DMPA) and 1-α-dimyristoylphosphatidylcholine with perdeuterated acyl chains (DMPC-$d_{54}$) were obtained from Avanti Polar Lipids, Inc. (Birmingham, AL) and used without further purification. Ferricytochrome *c* (Sigma VI Horseheart) was purified by chromatography through a CM-cellulose column according to the procedure of Brautigan et al. (32). The integrity of the ferricytochrome *c* was verified by visible spectroscopy. The multilayer dispersions of DMPA were prepared by first heating 10 mg of the sodium salt of the lipid in 1 ml water or 0.10 M phosphate buffer adjusted to either pH 4.0 or 7.0 to 65°C (above the gel to liquid crystalline transition, $T_m$) for 10 min and then mixing the dispersion mechanically. Thorough mixing and hydration was assured by multiple cycling of the sample temperatures through $T_m$ and by constant agitation. The calcium DMPA samples were prepared by adding a two- or threefold excess of calcium chloride to the sodium DMPA gel. The samples were then heated above 65°C and mechanically agitated while warm. After sealing both the sodium and calcium DMPA samples in glass capillary tubes, the multilayers were compacted in a hematocrit centrifuge. In cases where the lipid samples were gelatinous and did not easily compact, the dispersions were centrifuged in a Beckmann Ultracentrifuge for 20 min at 80,000 *g*. Samples were stored in a refrigerator at 2–5°C for at least 24 h before recording the spectra.

The mixed DMPA and deuterated DMPC-$d_{54}$ samples were dissolved in spectral grade chloroform. After the solvent was evaporated under a stream of nitrogen at 40°C, final traces of chloroform were removed under vacuum. A quantity of 0.10 M phosphate buffer adjusted to either pH 4.0 or 7.0 was added to the lipid mixture and thorough hydration was assured by four or five freeze-thaw cycles in which the sample was frozen in liquid nitrogen and thawed in water above 60°C. Subsequent treatment followed the same procedure described above for the pure DMPA samples.

Ferricytochrome *c*—DMPA and mixed lipid bilayers were reconstituted by adding the protein to the dispersed sodium DMPA or DMPA/DMPC-$d_{54}$ gel after it had cooled to room temperature. The sample was then mechanically agitated at room temperature without further heating. The calcium-lipid protein dispersions were formed by adding two- to threefold excess calcium chloride to the lipid sample containing both sodium DMPA or DMPA/DMPC-$d_{54}$ and protein; samples were further mixed at ambient temperatures. If ferricytochrome *c* is added to the sodium DMPA gel before adding the calcium salt, the dispersion attains a uniformly pink color. However, when the calcium salt is added before ferricytochrome *c*, the protein remains in the solution above the colorless lipid. The pink color of the DMPA-ferricytochrome *c* complex and the mixed DMPA-DMPC lipid ferricytochrome *c* complex disappears when the mixture is heated above 50°C. Subsequent manipulation of the samples reconstituted with ferricytochrome *c* followed the procedures used for the liposomal DMPA dispersions.

Raman spectra were observed generally as a function of temperature at 1.0°C intervals from 5° to 70°C. The specific temperature range varied between experiments. A thermostatted bath circulated heat exchanged fluid through a thermoelectrically controlled sample holder, which also housed the thermocouple used for monitoring the bath temperature. A separate solid state temperature-sensitive device controlled the power supplied to the thermoelectric temperature regulator. The intensity of the 514.5-nm laser excitation, obtained from a Spectra Physics 165 Ar laser, ranged from 30–75 mW at the sample for the various experiments. The scattered light was collected with a Spex Triplemate spectrograph at a spectral resolution of ~5–6 $cm^{-1}$ for the 1,200 line/mm grating and at a resolution of ~10–12 $cm^{-1}$ for the 600 line/mm grating. A 1,200 line/mm grating was used to span the 3,100 $cm^{-1}$ to 2,800 $cm^{-1}$ region for the single lipid component systems, while a 600 line/mm grating permitted the diode array to span the 3,100 $cm^{-1}$ to 2,000 $cm^{-1}$ area to record simultaneously both the C-H and C-D stretching mode spectral regions. Spectra were detected with a EG&G EG&G Princeton Applied Research (Princeton, NJ) thermoelectrically cooled, intensified silicon diode array. Raman emission, as well as temperature bath control, were recorded and controlled, respectively, with a DEC PDP 11/23 based laboratory computer system. Spectral files were transferred to a DEC PDP 11/84 computer for both data storage and spectral manipulation.

Calorimetric data were obtained with a Hart Scientific (Provo, UT) differential scanning calorimeter, comprised of the following components: a model 3705 adiabatic controller, a model 3706 temperature scan controller, a model 1701 Microtherm analogue multiplexer and preamplifier, and a model 707 digital voltmeter. The thermograms for each sample were measured as functions of increasing and decreasing temperature with scan rates of 10°C per hour. Phase transition temperatures, widths, and thermodynamics were determined from the calorimetric and spectral data using a two state model for lipid phase transitions (33). The reported uncertainties in $T_m$ and $\Delta T$ are for the 95% confidence level assuming the number of degrees of freedom are the number of points within the transition interval.

## RESULTS AND DISCUSSION

## A. Cation complexes of lipid systems

### Calcium and sodium dimyristoylphosphatidic acid

Although the Raman 3,100–2,800 $cm^{-1}$ C-H stretching mode region is quite complex, changes in the spectral intensity as a function of bilayer perturbation reflect both inter- and intramolecular changes within the hydrophobic region of the membrane. Specifically, unique Fermi resonance interactions and their resultant intensity distributions are dependent upon chain conformation and, for example, reflect increasing intrachain disorder for an increase in bilayer temperature (25). The Raman spectral temperature profiles for the calcium DMPA multilayers at pH 7 indicate no distinct phase transition corresponding to a gel to liquid crystalline phase change occurring in the experimentally examined range of 20–80°C. Fig. 1 *a* is a topological plot of the C-H stretching mode region. The axes in the plane are the wavenumber and temperature, while the intensity of the Raman scattering is graphed on the out-of-plane axis. As shown in this plot, the intensity of the 2,935 $cm^{-1}$ spectral region increases gradually with temperature but the 2,880 $cm^{-1}$ region remains relatively unchanged. The change in the 2,935 $cm^{-1}$ feature, assigned to part to a Fermi resonance component of the acyl chain terminal methyl symmetric stretching mode, implies a perturbation at the bilayer center affecting the intensity distributions of the 2,872 and 2,935 $cm^{-1}$ Fermi doublet (25). The peak intensity ratios of the 2,935 $cm^{-1}$ and the 2,880 $cm^{-1}$ features, $I_{2935}/I_{2880}$, displayed in Fig. 1 *b*(*A*), increase with rising temperature without the abrupt change that is indicative of a phase transition. This spectral parameter is a measure of primarily the interchain disorder with some contribution from intrachain trans/gauche conformer changes. Thus, the calcium DMPA sample shows increasing inter- and intramolecular chain disorder with increasing temperature, but does not form the disordered liquid crystalline phase at temperatures below 75°C. The more pure lateral chain packing parameter, $I_{2850}/I_{2880}$, only increases gradually over the 20–80°C temperature range, as shown in Fig. 1 *b*(*B*). (These stretching mode peak height intensity ratios are plotted in the figures as $I_{\text{disordered}}/I_{\text{ordered}}$.)

The total intensity of Raman scattering over a vibrational mode is a function of the number of molecular scatterers in the exciting beam and the polarizability change of the molecule incurred by the vibrational displacement coordinate. Because the 3,000 $cm^{-1}$ spectral region represents a complex manifold of vibrational levels, we find it useful to monitor the relative total integrated intensity, *I*, of the Raman emission over the 2,800–3,100 $cm^{-1}$ interval. Fig. 1 *b*(*C*) displays a gradual increase over the 20–80°C temperature range, demonstrating no change in either the packing density of the sample or alteration in the polarizability gradients of the acyl chain methylene stretching modes that usually accompany gel to liquid crystalline phase transitions. The differential scanning calorimetric profile (data not shown) of calcium DMPA at pH 7 indicates a very weak endothermic transition at ~53°C with an enthalpy of

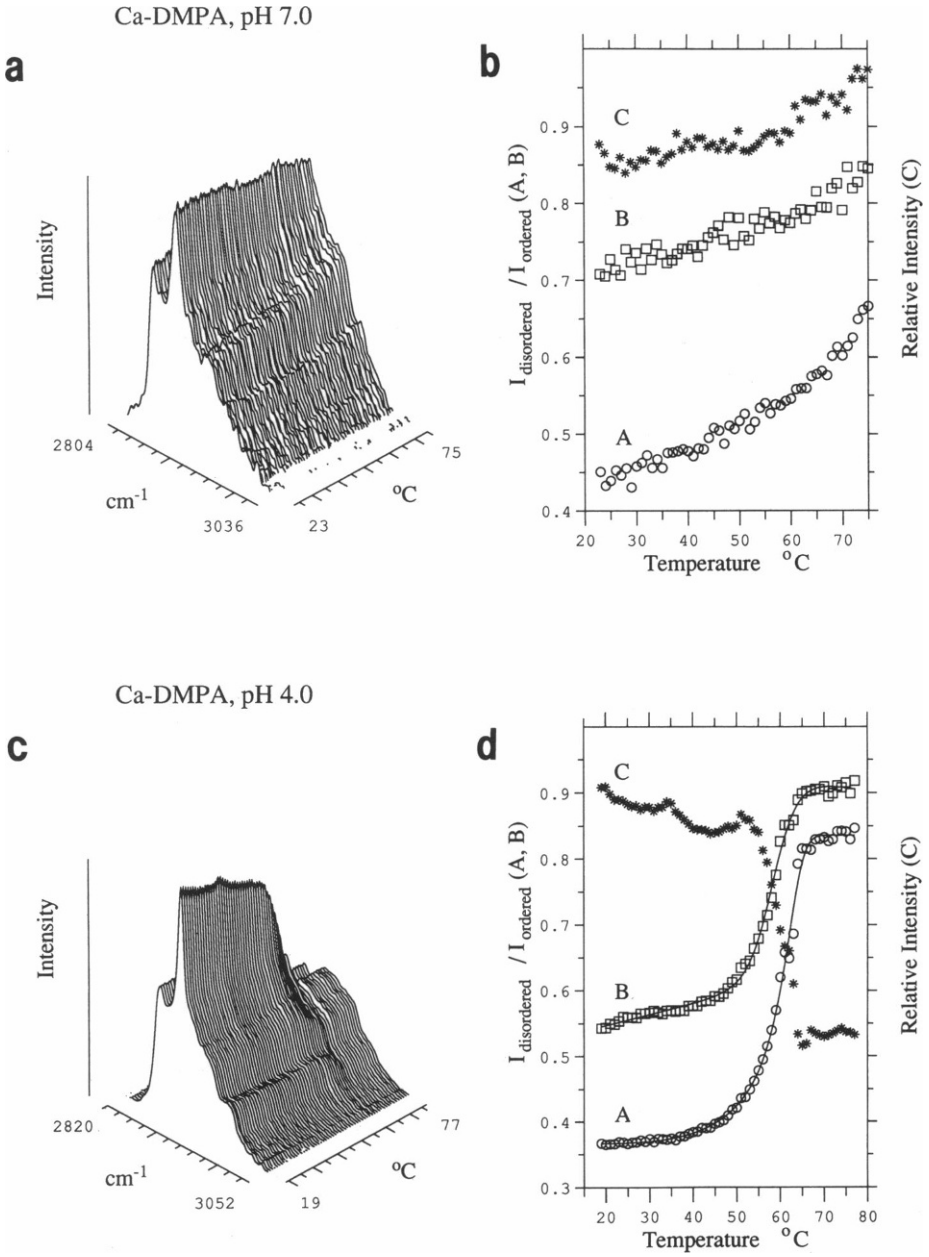


FIGURE 1 Raman spectra of calcium DMPA as a function of temperature; (*a*) Raman CH stretching mode region (2,800–3,000 $cm^{-1}$) at pH 7.0. (*b*) Peak height intensity ratios: *A*, $I_{2935}/I_{2880}$; *B*, $I_{2850}/I_{2880}$; and *C*, the relative integrated intensity over the CH stretching mode region at pH 7.0. (*c*) Raman CH stretching mode region (2,800–3,000 $cm^{-1}$) at pH 4.0. (*d*) Peak height intensity ratios; *A*, $I_{2935}/I_{2880}$; *B*, $I_{2850}/I_{2880}$; and *C*, the relative integrated intensity over the CH stretching mode region at pH 4.0. The lines were calculated using a two state model for lipid transitions (31) to fit the experimental points in A and B.

<0.8 KJ/mol. The lack of a definite gel to liquid crystalline phase transition in the pH 7.0 calcium DMPA complex confirms the results of Kouaouci et al. (4) and the studies of Liao and Prestegard (16), in which no distinct phase transition is detected by either Raman spectroscopy or calorimetry, respectively.

The approximate equilibrium dissociation constants for the phosphate moiety of DMPA are $pK_1 = 3.5$ and $pK_2 = 9$ (19). Under our experimental conditions of pH 4.0 and pH 7.0 the number of hydrogens dissociated, or degree of dissociation, in DMPA is nearly 0.5 at the low pH and 1 at pH 7.0. It is expected then, that at pH 4.0 the lipid head group will be more loosely coordinated than at pH 7.0 where one proton is replaced with a cation.

This conjecture is confirmed in the pH 4.0 calcium DMPA system which, in contrast to the pH 7.0 case, undergoes a distinct gel to liquid crystalline phase transition at ~60°C. Fig. 1 *c* presents for this system the topological plot of the C-H stretching mode region. The derived plot of the peak intensity ratio $I_{2935}/I_{2880}$ in Fig. 1 *d*(*A*) shows the high degree of order that exists in the calcium DMPA gel state before the main phase transition at 60.0 ± 0.3°C. This high degree of order is particularly evident in the peak intensity ratio $I_{2850}/I_{2880}$ which is ~0.57 at gel phase temperatures (Fig. 1 *d*[*B*]). This low value is suggestive of the orthorhombic or monoclinic form for the acyl chain subcell analogous to that found in crystalline DPPC dihydrate (34). In addition to the highly ordered value for the $I_{2850}/I_{2880}$ parameter, the $CH_2$ deformation region shows a feature at 1,420 $cm^{-1}$, also an indication of orthorhombic or monoclinic packing characteristics of the acyl chain matrix (35). The phase transition temperature, $T_m$, determined by the $I_{2850}/I_{2880}$ ratio is 58.5 ± 0.5 °C (Table 1) which is 1.5 degrees lower than the $T_m$ of 60.0 ± 0.3°C indicated by the $I_{2935}/I_{2880}$ peak intensity ratio. $T_m$ values determined by fitting a two state model to temperature profiles with this density of points and quality of data have estimated errors of <0.3–0.5°C in $T_m$. A difference of 1.5°C in $T_m$ is significant and indicates that different processes are responsible for the change in this spectral parameter. Thus, the disorder/order transition arising from decreased chain-chain interactions appears at a statistically lower temperature compared with the overall disorder of the acyl chains derived from both interchain and intrachain processes. That is, the decrease in order due to interchain interactions occurs before the introduction of the gauche conformers required to define the liquid crystalline phase. A plot of the relative total integrated intensity over the C-H stretching spectral region also indicates the phase transition by the decrease in scattering intensity following $T_m$ (Fig. 1 *d*[*C*]). If the two state theory is applied to the relative total integrated intensity curve, a transition temperature of 60.6 ± 0.5°C is obtained which has a width of 1.7 ± 0.5°C. This $T_m$, derived from the integrated scattering intensity, is close to the $T_m$ (60.0 ± 0.3°C) derived from the combination inter and intrachain disorder parameter, $I_{2935}/I_{2880}$, suggesting a correlation of the trans/gauche isomerization with the highly cooperative bilayer change in molecular polarizability and number of scattering centers. The DSC data (not shown) of the pH 4 calcium-DMPA multilayers also show an endothermic event at 60–62°C. The enthalpy change is ~8 KJ/mol for the multilamellar vesicles. Unilamellar vesicles of pH 4.0 calcium-DMPA showed a less complex endothermic transition at 62°C with a larger enthalpy change of 10.5 KJ/mol. We also find the enthalpy change at pH 4.0 in the sodium-DMPA system is 19.8 KJ/mol at 51°C. The small endothermic transitions in the pH 7 calcium DMPA system may be attributed to small amounts of sodium DMPA which still exist in equilibrium with calcium DMPA. Hauser and Dawson (36) have examined the replacement of sodium ions for calcium ions bound to monolayers of DMPA on a water air interface and have determined the equilibrium constant for such a replacement.

The Raman spectral properties of the sodium DMPA

**TABLE 1 Raman spectral parameters for multilamellar vesicles composed of the sodium and calcium salts of dimyristoylphosphatidic acid and ferricytochrome c complexes at pH 4 and pH 7**

| | | Peak height intensity ratios* | | | | | | | |
|---|---|---|---|---|---|---|---|---|---|
| | | $I_{2935}/I_{2880}$ | | | | $I_{2850}/I_{2880}$ | | | |
| Sample | pH | Gel | Liquid crystalline | $T_m$°C‡ | $\Delta T$°C‡ | Gel | Liquid crystalline | $T_m$°C‡ | $\Delta T$°C‡ |
| Na-DMPA | 7 | 0.45 | 0.75 | 49.3 ± 0.3 | 0.5 ± 0.3 | 0.79 | 0.91 | 49.9 ± 0.7 | 1.1 ± 0.5 |
| | 4 | 0.48 | 0.86 | 51.2 ± 0.3 | 0.5 ± 0.3 | 0.90 | 1.14 | 51.3 ± 0.3 | 0.6 ± 0.3 |
| | 1 | 0.46 | 0.92 | 47.3 ± 0.6 | 1.0 ± 0.6 | 0.66 | 0.96 | 47.3 ± 0.4 | 0.2 ± 0.3 |
| Ca-DMPA | 7 | 0.45 | — | — | — | 0.73 | — | — | — |
| | 4 | 0.40 | 0.84 | 60.0 ± 0.3 | 3.2 ± 0.3 | 0.59 | 0.91 | 58.5 ± 0.5 | 2.9 ± 0.4 |
| Na-DMPA + | 7 | 0.48 | — | — | — | 0.78 | — | — | — |
| Ferricytochrome *c* | 4 | 0.33 | — | — | — | 0.80 | — | — | — |
| Ca-DMPA + | 7 | 0.35 | — | — | — | 0.76 | — | — | — |
| Ferricytochrome *c* | 4 | 0.33 | — | — | — | 0.71 | 0.95 | 58.8 ± 4.0 | 6.3 ± 3.2 |

*The peak height intensity ratios for the gel and liquid crystalline states are values of the two state fitted curve taken 15°C below and above the phase transition temperature $T_m$, respectively, for those systems fit by the two state theory. Other peak height intensity ratios are listed for either 20° or 60°C.

‡The main phase transition temperatures $T_m$ and the width of the phase transition $\Delta T$ were determined by fitting a theoretical line derived from a two state model for lipid phase transitions (33) to the peak height ratio data. The uncertainties are 95% confidence levels assuming the degrees of freedom are the number of data points within the transition interval.

system at both values of pH (pH 4 and pH 7) are characteristic of multilamellar assemblies which have gel to liquid crystalline phase transition temperatures of ~50°C (Table 1). The topological presentation of the Raman spectra of sodium DMPA at pH 7 appears in Fig. 2 *a*; the peak height intensity ratios of $I_{2935}/I_{2880}$ and $I_{2850}/I_{2880}$ and the relative integrated intensities appear in Figs. 2 *b*(*A*), 2 *b*(*B*), and 2 *b*(*C*), respectively. The large integrated intensity decrease of the Raman signal that occurs at 30–35°C probably follows the breaking up of large multilamellar liposomes to form smaller liposomal assemblies. The peak height ratios do not show any

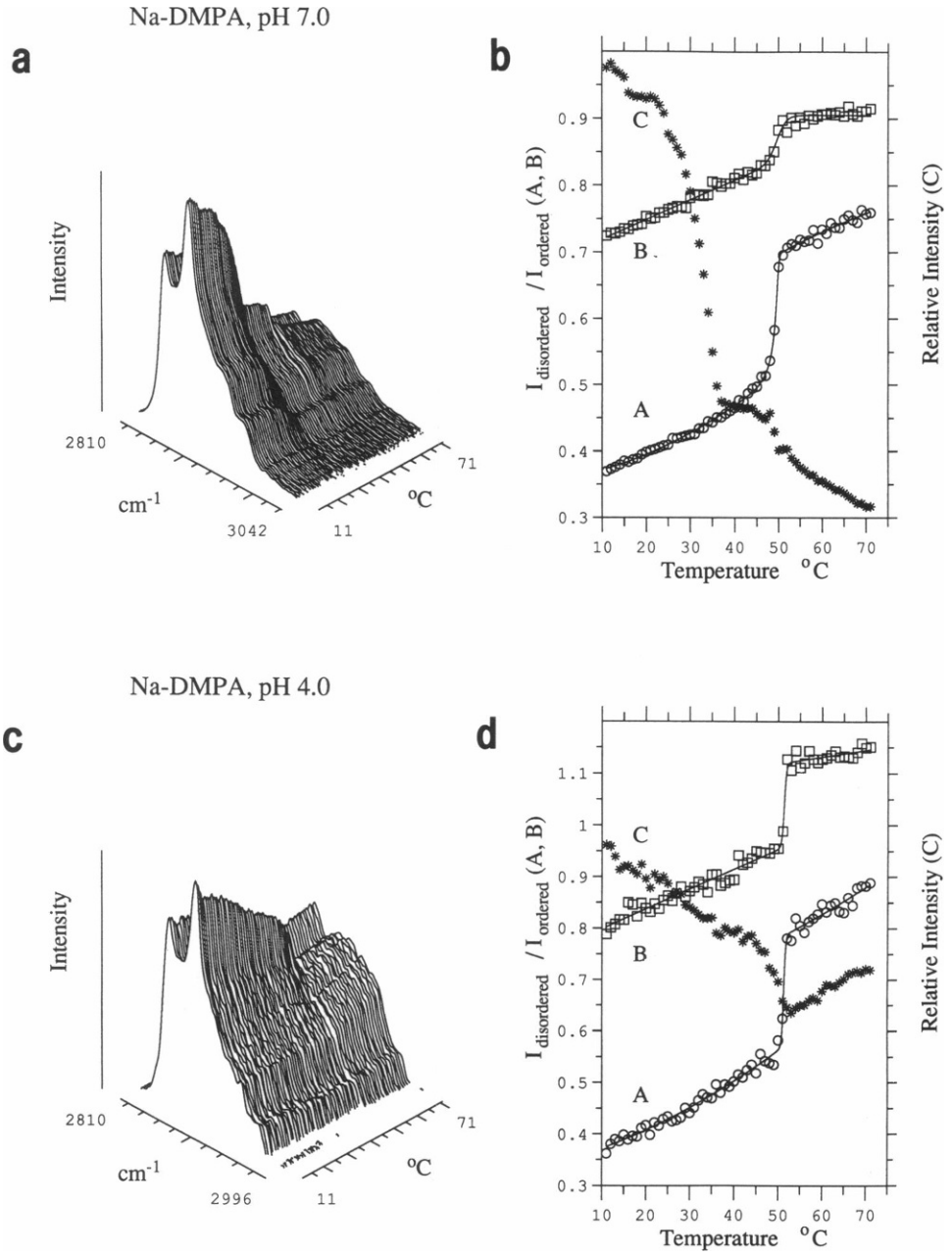


FIGURE 2 Raman spectra of sodium DMPA as a function of temperature; (*a*) Raman CH stretching mode region (2,800–3,000 $cm^{-1}$) at pH 7.0. (*b*) Peak height intensity ratios: *A*, $I_{2935}/I_{2880}$; *B*, $I_{2850}/I_{2880}$; and *C*, the relative integrated intensity over the CH stretching mode region at pH 7.0. (*c*) Raman CH stretching mode region (2,800–3,000 $cm^{-1}$) at pH 4.0. (*d*) Peak height intensity ratios; *A*, $I_{2935}/I_{2880}$; *B*, $I_{2850}/I_{2880}$; and *C*, the relative integrated intensity over the CH stretching mode region at pH 4.0. The lines were calculated using a two state theory (31) to fit the experimental points in *A* and *B*.

significant change throughout the 30–40°C temperature range of the large intensity variation which would indicate a modulation of the gel state order. Also, there is no total intensity change throughout the gel state temperature range when examining, spectroscopically, 100-nm diam unilamellar vesicles rather than the multilamellar structures of sodium DMPA at pH 7.0. The values of $T_m$ determined using both peak height ratios, $I_{2935}/I_{2880}$ and $I_{2850}/I_{2880}$, are nearly the same for the unilamellar systems, suggesting that in the sodium DMPA system the interchain and the gauche/trans order-disorder transitions occur at the same temperature.

The decrease in the Raman scattering intensity of the sodium DMPA system at pH 4.0 throughout the gel phase, as shown in Fig. 2 *c*, is not as dramatic as that in the previously described pH 7.0 system. The total scattering intensity does decrease with temperature in the gel phase, suggesting that at pH 4 the size of the sodium DMPA liposomes is dependent upon temperature, but not to the extent of the pH 7.0 liposomes. The disorder/order parameters in the gel phase are slightly larger than the corresponding values in the pH 7.0 system, indicating a more disordered liposome. The bilayer headgroup is less tightly coordinated by cations due to the smaller fraction of dissociation at the more acidic pH. The crystal structure data of Harlos et al. (15) for the sodium DMPA bilayers show hydrogen bonding and cation coordination between neighboring phosphate groups both within and between lipid layers, suggesting that head group interactions are important in the determination of the phospholipid packing in hydrated DMPA systems. Eibl and others (18, 19, 37) proposed DMPA models involving hydrogen bonding in the head group region to interpret the variation of $T_m$ as a function of pH. They found, using fluorescence probes and light scattering techniques, that the $T_m$ occurs at a higher temperature for pH 4.0 sodium DMPA than for either this system at pH 7.0 or at pH 1.0, an observation consistent with our results. The Raman spectroscopic results for the sodium and calcium DMPA complexes are summarized in Table 1.

The stronger coordination of calcium with the lipid phosphate head group compared with sodium can lead to several consequences when calcium replaces sodium as cation. Adjacent lipid headgroups may be held together more securely leading to a more stable gel phase thereby increasing the $T_m$ for the gel to liquid crystalline phase transition. Calcium participates more strongly than sodium in coordination between headgroups from adjacent lipid bilayers, decreasing the water content between multilayer shells. Liao and Prestegard (16) found by low angle x-ray scattering that calcium and cadmium DMPA have shortened bilayer repeat distances compared with those of comparable choline phospholipids. They suggest the possibility of cation coordination bridging bilayers in DMPA. This coordination is pH dependent due to the dissociation of DMPA. At pH 7, where the degree of dissociation for the phosphate is one, the coordination of one calcium or other cation for each headgroup is permitted, creating a tight lattice structure resistant to a phase transition. As the pH is reduced, proton association now competes with cation coordination reducing both the possible bilayer bridging and strong cation coordination between headgroups. This qualitatively accounts for the observation of a gel to liquid crystalline phase transition in calcium DMPA at pH 4.0 and the absence of a phase transition at pH 7.0.

### 1:1 mole ratio mixtures of DMPA and DMPC-$d_{54}$

Kouaouci et al. (4) observed by Raman spectroscopic techniques that the addition of calcium ion to the 1:1 mixed lipid systems, DMPA/DMPC-$d_{54}$ or DMPC/DMPA-$d_{54}$, induced lateral segretation of the lipid components of pH 7.5. The main transition temperature, $T_m$, of the mixture in the presence of calcium was dependent upon which component was measured. The phosphatidic acid component did not exhibit a distinct phase transition; but the phase transition of the phosphatidylcholine, although broader than that of the pure lipid, occurred at nearly the same temperature as the pure lipid. Their finding of lipid segregation with the calcium cation is in contrast to their observation of no lipid segregation in pH 7.5 samples in which sodium was the cation. Our studies of the DMPA/DMPC-$d_{54}$ system in which sodium is the cation also indicate no distinct lipid segregation at either pH 4.0 or pH 7.0. Figs. 3 *a* and *c*, show the topological plots of the Raman spectra of the CH and CD stretching mode regions, respectively, as a function of temperature of 1:1 mixed sodum DMPA/DMPC-$d_{54}$ at pH 7.0. In the accompanying Figs. 3 *b* and *d*, the peak intensity ratios of the CH stretching mode and the linewidths of the CD region both indicate a common broad phase transition at ~35°C (Table 2). The $T_m$ for DMPC-$d_{54}$ is 18°C (30). In addition to this phase transition, the topological plots illustrate increases in the Raman intensity in both the C-H and C-D stretching mode regions of the spectra at ~50°C, a temperature close to that of the normal $T_m$ of sodium DMPA. The peak height intensity ratio $I_{2850}/I_{2880}$ (Fig. 3 *b*[*B*]), primarily a measure of chain-chain or lateral disorder, increases gradually for DMPA in this mixed lipid system with a broad transition ($\Delta T$ = 8.7°C) at 34.6 ± 3.5°C. The CH parameter, containing intrachain disorder superimposed on existing lateral disorder, $I_{2935}/I_{2880}$, (Fig. 3 *b*[*A*]) of DMPA has a relatively narrow phase transition ($\Delta T$ = 1.7°C) at 37.2 ± 0.7°C.

TABLE 2 **Raman spectral parameters for multilamellar vesicles composed of ferricytochrome c complexes with sodium and calcium salts of 1:1 mixtures of dimyristoylphosphatidic acid and dimyristoylphosphatidylcholine-$d_{54}$ at pH 4 and pH 7**

| | | Peak height intensity ratios, DMPA* | | | | | | |
|---|---|---|---|---|---|---|---|---|
| | | $I_{2935}/I_{2880}$ | | | $I_{2850}/I_{2880}$ | | | |
| Sample | pH | Gel phase | Liquid crystalline | $T_m$°C‡ | $\Delta T$°C‡ | Gel phase | Liquid crystalline | $T_m$°C‡ |
| Na-DMPA + DMPC-$d_{54}$ | 7 | 0.46 | 0.88 | 37.2 ± 0.7 | 1.7 ± 0.5 | 0.80 | 0.96 | 34.6 ± 3.5 |
| | 4 | 0.41 | 0.85 | 39.6 ± 1.5 | 3.7 ± 1.2 | 0.75 | 0.85 | — |
| Ca-DMPA + DMPC-$d_{54}$ | 4 | 0.51 | 0.78 | 49.8 ± 1.1 | 1.9 ± 0.8 | 0.75 | 0.95 | — |
| Ca-DMPA + DMPC-$d_{54}$ + Ferricythchrome *c* | 7 | 0.50 | 0.71 | 45.3 ± 1.2 | 2.0 ± 1.2 | 0.72 | 0.80 | — |
| | 4 | 0.47 | 0.75 | 45.1 ± 1.2 | 14.2 ± 1.0 | 0.72 | 0.85 | — |

*The peak height intensity ratios for DMPA and the linewidths for DMPC-$d_{54}$ for the gel and liquid crystalline states are values of the two state fitted curve taken 15°C below and above the phase transition temperature $T_m$, respectively, for those systems fit by the two state theory. Other peak height ratios and linewidths are listed for either 15° or 60°C.

Similarly, the CD intra-chain disorder parameter, $\Delta\nu_{1/2}$, has a relatively narrow ($\Delta T$ = 1.7°C phase transition with $T_m$ at 34.4 ± 1.2°C, while the inter-chain or lateral disorder parameter, $\Delta\nu_{7/8}$, displays a broad ($\Delta T$ = 4°C) phase transition at 35.9 ± 3.4°C. From these data we may postulate a model of a thoroughly mixed lipid system in which the bilayer disorder arising predominantly from guache/trans conformational changes is induced thermally over a relatively narrow temperature range nearly midway between the $T_m$'s of each pure component. Because the pure lateral transition monitored by the $I_{2850}/I_{2880}$ index occurs at a lower $T_m$ and has a broader temperature range than the $I_{2935}/I_{2880}$ transition, the lipid lattice apparently expands before the introduction of gauche conformers along the acyl chains. The values for $T_m$ derived from the linewidths of DMPC-$d_{54}$ are essentially the same for both the inter- and intra-chain disorder/order parameters. However, the $\Delta T$'s of the disorder parameters, $\Delta\nu_{7/8}$ and $I_{2850}/I_{2880}$, corresponding to lateral chain-chain interaction are considerably larger than the $\Delta T$'s for the parameters, $\Delta\nu_{1/2}$ and $I_{2935}/I_{2880}$, related to the gauche/trans conformation ratio, indicating the importance of contributions from the various headgroup populations with the variety of nearest neighbor interactions. That is, even though the binary lipid system is mixed without observable lateral separation, there exists a distribution of headgroup interactions arising from the local nonuniform distribution of lipids. These nonuniform distributions could perhaps explain the high temperature inflection seen in Fig. 3 *b*(*C*) and the intensity change in the same temperature region in Fig. 3 *c*.

The 1:1 mole ratio mixed DMPA, DMPC-$d_{54}$ lipid with the sodium cation at pH 4.0 exhibits somewhat similar behavior to the pH 7.0 sample. The Raman spectra, linewidths, and peak intensity ratios are analogous to those shown in Fig. 3. The parameters related to intra-chain disorder, $\Delta\nu_{1/2}$ and $I_{2935}/I_{2880}$, (Table 2) indicate broader phase transitions than in the pH 7.0 system and increased $T_m$ values close to 40°C, still a $T_m$ between $T_m$'s of 18°C and 51.2°C for the two pure components in the binary mixture. The parameters reflecting lateral chain-chain bilayer disorder, $\Delta\nu_{7/8}$ and $I_{2850}/I_{2880}$ reflect increases in disorder at temperatures above 40°C. The small degree of dissociation ($\sim$0.5) of DMPA at pH 4.0 must permit the DMPA and DMPC head groups to interact more strongly than when one DMPA hydrogen is replaced by a sodium ion at pH 7.0. Both intra- and interchain disorder parameters show the increased values of $T_m$ for the DMPC-$d_{54}$; but while the trans/gauche isomerization parameter, $I_{2935}/I_{2880}$, of DMPA indicates the elevated $T_m$, the C-H stretching mode parameter of lateral disorder, $I_{2850}/I_{2880}$, does not indicate a corresponding phase transition.

At a pH of 4.0 the multilamellar vesicles composed of DMPA and DMPC-$d_{54}$ with an excess of calcium showed no distinct evidence for lipid segregation. The Raman spectral topological plots, linewidths, and peak intensity ratios as a function of temperature are shown in Fig. 4. The peak intensity ratio $I_{2935}/I_{2880}$ of calcium DMPA (Fig. 4 *b*[*A*]) indicates a phase transition at 49.8 ± 1.1°C, compared with 60.0°C for pure calcium DMPA bilayers at this pH. The liquid crystalline phase $I_{2935}/I_{2880}$ intensity ratio for DMPA is <0.8, a value indicating a relatively ordered fluid phase. The peak ratio $I_{2850}/I_{2880}$ (Fig. 4 *b*[*B*]) increases gradually to $\sim$50°C and then decreases slowly with increasing temperature. A distinct phase transition is not apparent from this parameter. The DMPC-$d_{54}$ species in Fig. 4 *d*(*D*) and Fig. 4 *d*(*E*), also shows a phase transition. The $\Delta\nu_{1/2}$ profile shows a broad transi-

TABLE 2 (continued)

| Linewidth ($cm^{-1}$), DMPC-$d_{54}$* | | | | | | | | |
|---|---|---|---|---|---|---|---|---|
| $\Delta\nu_{1/2}$ | | | | $\Delta\nu_{7/8}$ | | | | |
| $\Delta T$°C‡ | Gel phase | Liquid crystal-line | $T_m$°C‡ | $\Delta T$°C‡ | Gel phase | Liquid crystal-line | $T_m$°C‡ | $\Delta T$°C‡ |
| 8.7 ± 3.8 | 40 | 51 | 34.4 ± 1.2 | 1.7 ± 1.3 | 14 | 18 | 35.9 ± 3.4 | 4.0 ± 2.5 |
| — | 42 | 67 | — | — | 12 | 17 | 41.5 ± 1.3 | 1.0 ± 1.3 |
| — | 40 | 54 | 44.2 ± 2.5 | 4.1 ± 2.3 | 12 | 22 | 47.3 ± 0.9 | 1.0 ± 0.9 |
| — | 38 | — | — | — | 18 | 26 | — | — |
| — | 37 | — | — | — | 13 | 12 | — | — |

*The main phase transition temperatures $T_m$ and widths of the phase transition $\Delta T$ were determined by fitting a theoretical line derived from a two state model for lipid phase transitions (33) to the peak height ratio data of the CH stretching mode region and to the linewidth of the CD 2,103 $cm^{-1}$ feature at $\Delta\nu_{1/2}$ and $\Delta\nu_{7/8}$ of the peak height. The uncertainties are 95% confidence levels assuming the degrees of freedom are the number of data points within the transition interval.

tion at 44.2 ± 2.5°C, whereas the $\Delta\nu_{7/8}$ temperature profile indicates a transition at 47.3 ± 0.9°C. These intramolecular and intermolecular parameters, respectively, imply in this case that the gauche/trans isomerization process drives the lattice expansion because the $T_m$ for $\Delta\nu_{1/2}$ occurs at the lower temperature. These variations in $T_m$ suggest that although the mixture is generally homogeneous, there is a dynamic distribution of do-

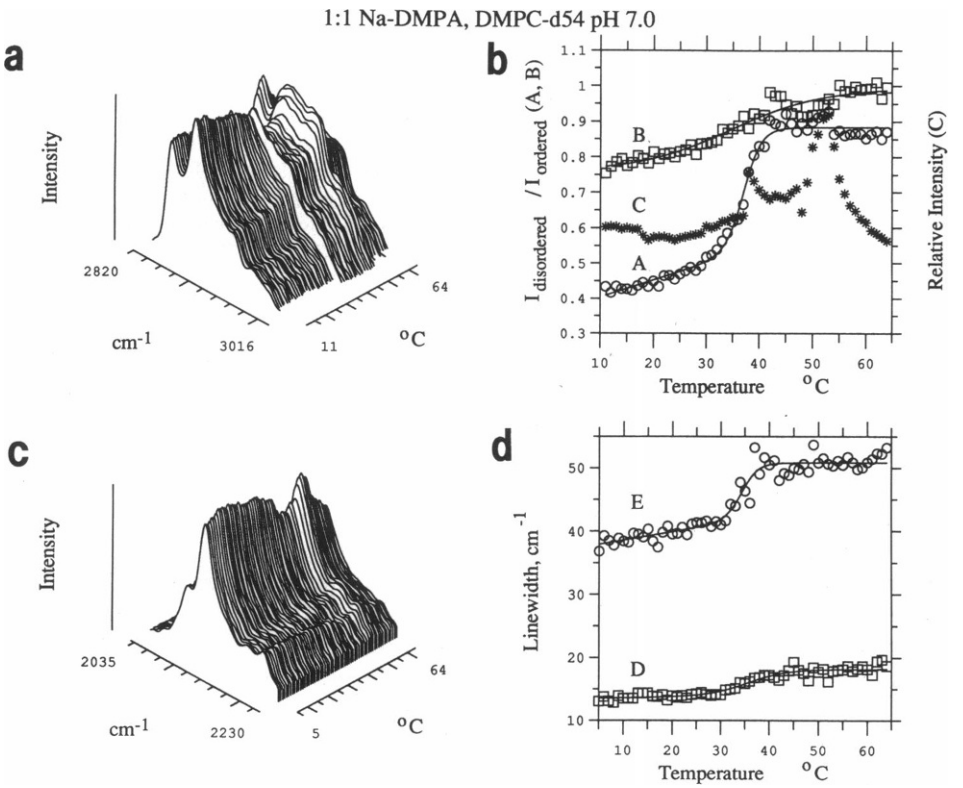


FIGURE 3 Raman spectra of the 1:1 mole ratio mixed lipid system of sodium DMPA and DMPC-$d_{54}$ at pH 7.0 as a function of temperature. (*a*) Raman CH stretching mode region (2,800–3,000 $cm^{-1}$) for the sodium DMPA species in the mixture. (*b*) Peak height intensity ratios; *A*, $I_{2935}/I_{2880}$; *B*, $I_{2850}/I_{2880}$; and *C*, the relative integrated intensity over the CH stretching mode region for the sodium DMPA species. (*c*) Raman spectra of the CD stretching mode region (2,000–2,250 $cm^{-1}$) for the DMPC-$d_{54}$ species in the mixture. (*d*) Linewidths of the $CD_2$ symmetric stretching modes at 2,103 $cm^{-1}$; *D*, $\Delta\nu_{7/8}$; and *E*, $\Delta\nu_{1/2}$. The lines were calculated using a two state theory (31) to fit the experimental points in *A*, *B*, *D*, and *E*.

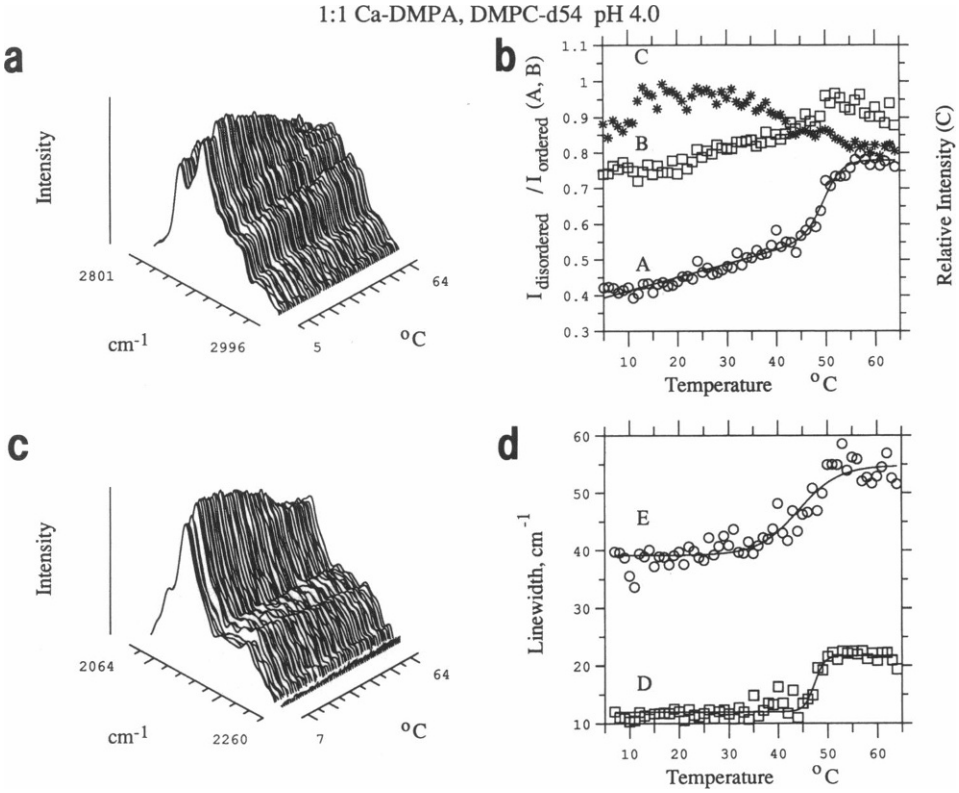


FIGURE 4 Raman spectra of the 1:1 mole ratio mixed lipid system of calcium DMPA and DMPC-$d_{54}$ at pH 4.0 as a function of temperature. (*a*) Raman CH stretching mode region (2,800–3,000 $cm^{-1}$) for the calcium DMPA species in the mixture. (*b*) Peak height intensity ratios; *A*, $I_{2935}/I_{2880}$; *B*, $I_{2850}/I_{2880}$; *C*, the relative integrated intensity over the CH stretching mode region for the calcium DMPA species. (*c*) Raman spectra of the CD stretching mode region (2,000–2,250 $cm^{-1}$) for the DMPC-$d_{54}$ species in the mixture. (*d*) Linewidths of the 2,103 $cm^{-1}$ $CD_2$ symmetric stretching modes; *D*, $\Delta\nu_{7/8}$; and *E*, $\Delta\nu_{1/2}$. The lines were calculated using a two state theory (31) to fit the experimental points in *A*, *B*, *D*, and *E*.

mains consisting of regions rich in DMPA and DMPC-$d_{54}$, respectively. Although these domains may be too small to display the distinct properties of laterally segregated pure lipid regions, their average thermal behavior is indicative of domains differing in lipid concentration. At pH 4.0 the multilamellar system is relatively ordered, probably due to the coordination of the calcium. However, because the degree of dissociation of DMPA is small, the calcium coordination is insufficient for completely separating the lipid components and forming calcium bridges between all the DMPA head groups.

## B. Ferricytochrome c interactions with lipid assemblies

### Ferricytochrome c complexes with sodium and calcium DMPA

The spontaneous Raman spectra of multilamellar vesicles composed of either sodium or calcium DMPA and ferricytochrome *c* (concentrations of the dispersions range from 507:1 to 970:1 lipid/protein mole ratio) show strong protein perturbations of the lipid structures with the possible exception of the pH 7.0 calcium DMPA system. Figs. 5, *a* and *b*, illustrate the results for sodium DMPA at pH 4.0, while Figs. 5, *c* and *d*, present the data for calcium DMPA at pH 4.0, in the same topological and intensity formats as the previous figures. The corresponding figures for the pH 7.0 species are similar to those illustrated for pH 4.0 except for those features indicated in the text. The ferricytochrome *c* complex with sodium DMPA multilayers is extremely temperature sensitive at both pH values, as demonstrated by Figs. 5, *a* and *b*. Above 40°C the Raman scattering becomes structureless, decreasing until it merges with the fluorescent emission, which increases with temperature and eventually saturates the detector. The sample loses its pink color, becoming colorless with a tinge of yellow. The integrated intensity of the Raman scattering, Fig. 5 *b*(*C*), begins to decrease abruptly for the pH 7.0 sample at ~26°C and for the pH 4.0 sample at ~38°C. Above ~40°C the peak height ratios become

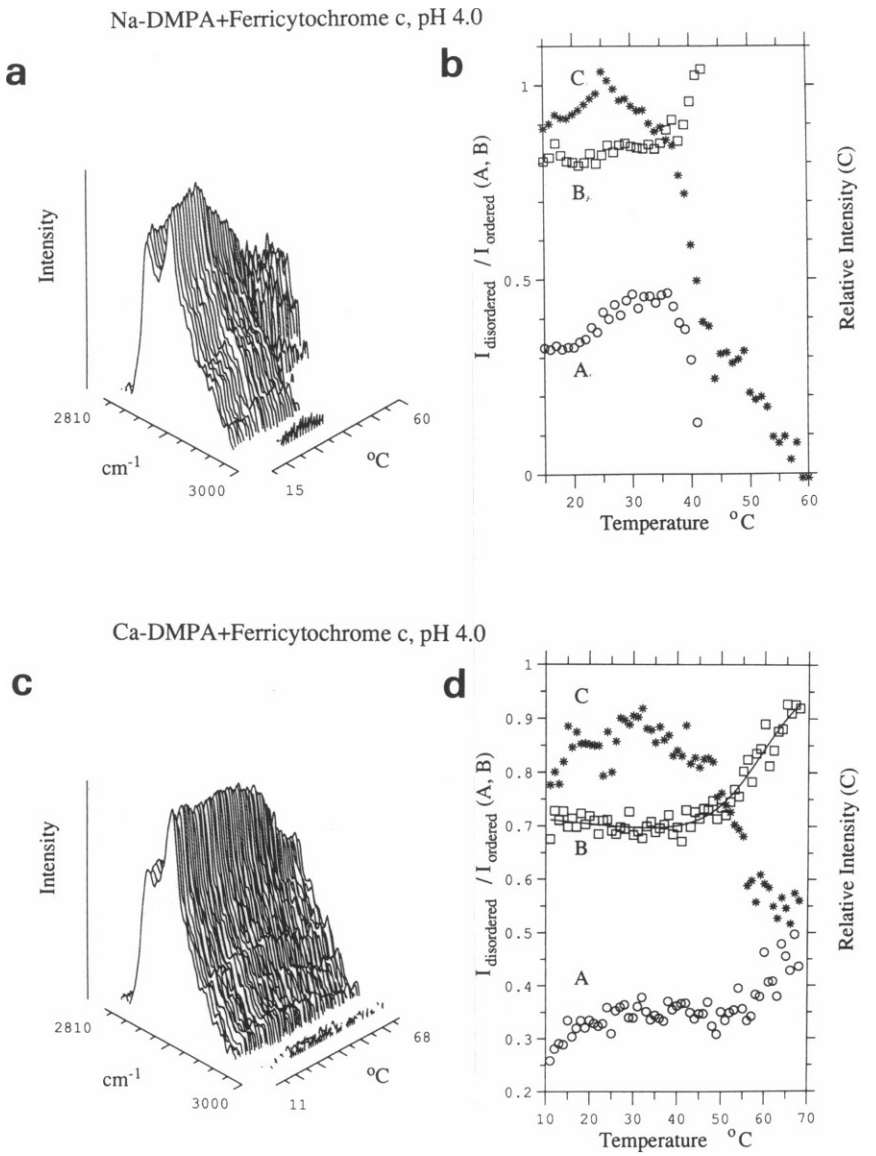


FIGURE 5 Raman spectra of the cation DMPA ferricytochrome *c* complexes at pH 4.0 as a function of temperature. (*a*) Raman CH stretching mode region (2,800–3,000 $cm^{-1}$) for the 900:1 lipid to protein mole ratio sodium DMPA ferricytochrome *c* complex. (*b*) Peak height intensity ratios: *A*, $I_{2935}/I_{2880}$; *B*, $I_{2850}/I_{2880}$; and *C*, the relative integrated intensity over the CH stretching mode region. (*c*) Raman spectra of the CH stretching mode region (2,800–3,000 $cm^{-1}$) for the 507:1 lipid to protein mole ratio calcium DMPA ferricytochrome *c* complex. (*d*) Peak height intensity ratios; *A*, $I_{2935}/I_{2880}$; *B*, $I_{2850}/I_{2880}$; and *C*, the relative integrated intensity over the CH stretching mode region.

less useful as the Raman scattering intensity vanishes, as shown in Figs. 5, *b*(*A*) and *b*(*B*). At low temperatures, however, the gel phase peak height ratios, $I_{2935}/I_{2880}$ and $I_{2850}/I_{2880}$, both indicate an ordered bilayer structure for the sodium DMPA-ferricytochrome *c* complex at both pH values. The disorder parameter $I_{2935}/I_{2880}$ increases with temperature for both pH samples until the lack of scattering intensity renders the parameter useless. The $I_{2850}/I_{2880}$ ratio, reflecting chain-chain interactions, remains relatively constant with increasing temperature at a moderately large value of ~0.8, indicating a comparatively high bilayer disorder, for the pH 4.0 sample (Fig. 5 *b*[*B*]), whereas the same parameter for the pH 7.0 sample continues to increase with temperature until the scattering intensity disappears. This temperature behavior indicates differences in the way the intermolecular and intramolecular parameters reflect disorder for the pH 4.0 and pH 7.0 samples. The parameter which contains some gauche/trans isomerization effects, $I_{2935}/I_{2880}$, varies similarly in both pH samples; however, the

pure intermolecular disorder parameter, $I_{2850}/I_{2880}$, which starts at a moderately high value for both samples at low temperatures, increases with temperature for the pH 7.0 sample but remains nearly constant for the pH 4.0 sample.

The calcium DMPA-ferricytochrome *c* complex is a more stable bilayer system than the analogous sodium complex. The Raman spectra of the 970:1 lipid/protein mole ratio pH 7.0 sample do not indicate a phase transition in the 15–75°C temperature range. Although there is a slight increase in gel phase disorder, the intensity ratios, $I_{2935}/I_{2880}$ and $I_{2850}/I_{2880}$, display no distinct phase transition, which is similar behavior to the protein free multilayers. As the temperature increased to 70°C, the integrated intensity decreased along with an increase in fluorescence suggesting that denaturation occurred. The samples became nearly colorless above 60°C. Although the protein is altered and presumed denatured above 60°C, this process appeared to have a lessened effect on the lipid bilayer order, as compared with the sodium DMPA-protein system, in Figs. 5, *a* and *b*. At pH 4 the 507:1 lipid/protein mole ratio calcium DMPA-ferricytochrome *c* complex appears to undergo a phase transition. Fig. 5 *c* illustrates Raman spectra of this species as a function of temperature. The peak height intensity ratios, $I_{2935}/I_{2880}$ and $I_{2850}/I_{2880}$, (Figs. 5, $d[A]$ and $d[B]$) increase between 50° and 70°C. The $T_m$ for this sample based upon the $I_{2850}/I_{2880}$ parameter is 58.8 ± 4°C, a value similar to 58.5°C observed for the system without protein. However, the width of this transition (6.3°C) is considerably broader than the transition in the system without the protein (2.9°C), emphasizing the reduced cooperativity of the melting process and the disordering effect the protein exerts upon the relatively ordered lipid bilayer.

### Ferricytochrome c complexes with 1:1 mole ratio lipid mixtures of sodium DMPA and DMPC-$d_{54}$

The Raman scattering from a pH 7.0 1:1 mole ratio binary mixture of sodium DMPA and DMPC-$d_{54}$ with ferricytochrome *c* at a concentration of 1000:1 lipid/protein mole ratio exhibits intensities and lineshapes which change considerably as a function of temperature. The peak height ratio $I_{2850}/I_{2880}$ of the sodium DMPA increases gradually with temperature without a discernable indication of a phase transition. The $I_{2935}/I_{2880}$ peak intensity ratio increases with temperature in two regions. The first is roughly from 15° to 25°C. The second region is in the range of 45°C, suggestively close to the $T_m$ of sodium DMPA and an indication of possible lateral segregation or domain formation. The linewidths of the 2,103 $cm^{-1}$ line of DMPC-$d_{54}$ are relatively constant until the temperature reaches 24°C, at which point both the $\Delta\nu_{1/2}$ and $\Delta\nu_{7/8}$ linewidth parameters fluctuate with temperature. The temperature at which these fluctuations begin is close to the $T_m$ (18°C) of DMPC-$d_{54}$. This overall behavior is consistent with a sample containing poorly defined domains, some rich in DMPA and others rich in DMPC, which can vary in size and composition as the experiment progresses. Because a constant temperature is maintained for more than a half hour at each temperature for which spectra are collected, the domain rich in zwitterionic DMPC-$d_{54}$ will contain the more mobile lipids which may allow lateral segregation. The integrated intensity curve of both species generally decreases from ~18 to 40°C with, however, a leveling and slight increase occurring in the 24–30°C interval. The integrated intensity of the C-H region of the DMPA species increases in intensity, suggesting an aggregation process, in the 46–49°C interval before leveling. This behavior is also consistent with an induction of domains by the protein in the ternary complex. Thus, interactions between ferricytochrome *c* and DMPA lead to domains of varying sizes and lipid concentrations, factors contributing to the fluctuations observed in the various parameters at temperatures above the $T_m$ for DMPC-$d_{54}$.

### Ferricytochrome c complexes with 1:1 mole ratio lipid mixtures of calcium DMPA and DMPC-$d_{54}$

The phase transition of the mixed lipid system of calcium DMPA and DMPC-$d_{54}$ with ferricytochrome *c* at pH 7.0 occurs at 45°C according to the CH stretching mode $I_{2935}/I_{2880}$ peak intensity ratio and the $\Delta\nu_{1/2}$ C-D 2,103 $cm^{-1}$ linewidth. The topological plots of the Raman spectra of both the CH and CD stretching modes as a function of temperature (Fig. 6) show no major changes in the linewidth or intensity parameters until the phase transition at 45°C. This single phase transition indicates that no lateral phase separation occurs in this system. Lipid phase segregation was observed, however, for the calcium DMPA-DMPC-$d_{54}$ system devoid of ferricytochrome *c* (4). The protein interaction with the lipid surface appears to inhibit competitively the interaction of calcium with the DMPA, the driving force for forming regions rich in calcium DMPA. The peak intensity ratio, $I_{2850}/I_{2880}$, of $<0.8$ also illustrates a relatively ordered population of DMPA lipids throughout the temperature range. This behavior is similar to the calcium DMPA pH 7.0 system in which no gel to liquid crystalline transition is observed. The phase transition in the calcium DMPA-DMPC-$d_{54}$-ferricytochrome *c* system is therefore due primarily to trans/gauche isomerization occurring within a laterally disordered chain lattice.

The 1:1 mixture of calcium DMPA and DMPC-$d_{54}$ multilayers reconstituted with ferricytochrome *c* at pH 4.0 also shows no evidence of lipid segregation. The

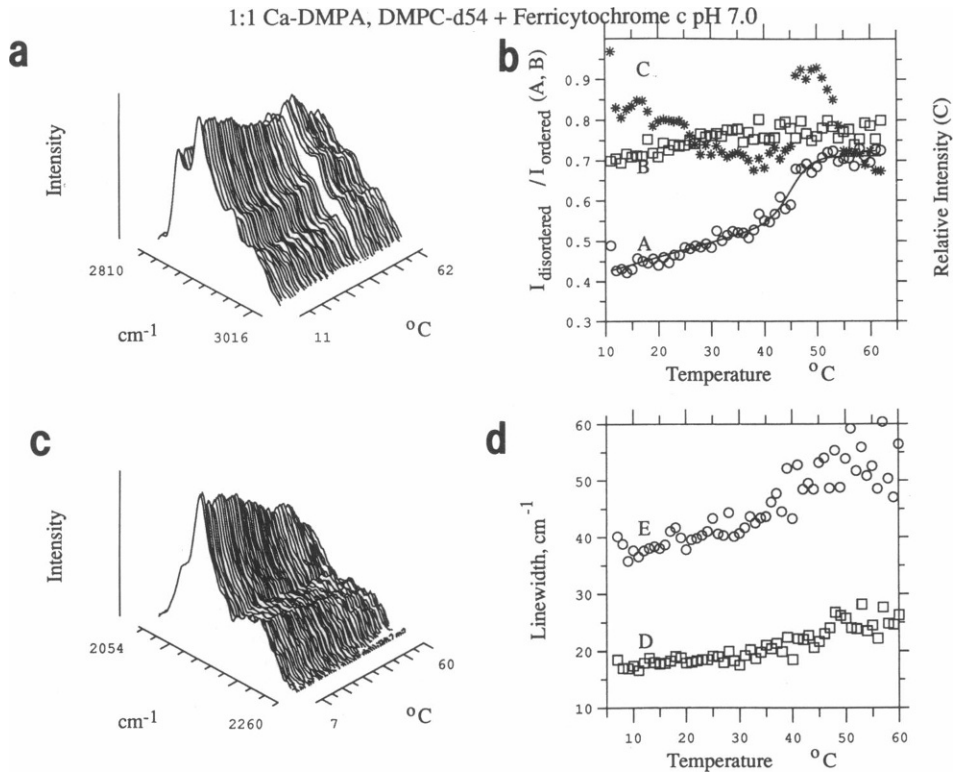


FIGURE 6 Raman spectra of the 1:1 mole ratio mixed lipid system of calcium DMPA and DMPC-$d_{54}$ with 500:1 lipid to ferricytochrome *c* mole ratio at pH 7.0 as a function of temperature. (*a*) Raman CH stretching mode region (2,800–3,000 $cm^{-1}$) for the calcium DMPA species in the mixture. (*b*) Peak height intensity ratios: *A*, $I_{2935}/I_{2880}$; *B*, $I_{2850}/I_{2880}$; and *C*, the relative integrated intensity over the CH stretching mode region. The line was calculated using a two state theory (31) to fit the experimental points in *A*. (*c*) Raman spectra of the CD stretching mode region (2,000–2,250 $cm^{-1}$) for the DMPC-$d_{54}$ species in the mixture. (*d*) Linewidths of the $CD_2$ symmetric stretching modes at 2,103 $cm^{-1}$; *D*, $\Delta\nu_{7/8}$; and *E*, $\Delta\nu_{1/2}$.

Raman spectra, peak height intensity ratios, and integrated intensities are similar to those features in the pH 7.0 species. Both the DMPA and DMPC-$d_{54}$ Raman spectral intensities increase gradually with temperature, reaching a maximum at 23°C then decline until the spectra become quite noisy at 50°C, where the protein begins to denature. The calcium DMPA peak intensity ratio $I_{2935}/I_{2880}$ indicates a phase transition at 43°C. Neither the $\Delta\nu_{1/2}$ linewidth of the 2,103 $cm^{-1}$ band of DMPC-$d_{54}$ nor the $I_{2850}/I_{2880}$ peak height ratio of DMPA show clear evidence of a phase transition. Lateral chain disorder appears to gradually increase throughout the temperature span.

## CONCLUSIONS

The thermotropic behavior of anionic phospholipid bilayer assemblies, such as DMPA, depends greatly on the pH, the nature of the counter ion and the presence of other perturbants in the system. The perturbant of interest in this study was the interaction of ferricytochrome *c* with the lipid systems composed of sodium and calcium complexes of DMPA and the 1:1 mole ratio mixture of DMPA and DMPC-$d_{54}$. To specify the protein interactions with the lipid structures, the various lipid assemblies were first examined devoid of protein. The pH and cation of the protein free systems determine many of the systems' thermotropic properties. The gel to liquid crystalline phase transition temperature $T_m$ in sodium DMPA is a function of pH; namely, the $T_m$ occurs at 51.2°C for pH 4.0, at 49.3°C for pH 7.0, and at 47.3°C for pH 1.0. Calcium DMPA at pH 4.0 displays its phase transition at 60.0°C; however, no phase transition was observed at pH 7.0. Mixed lipid systems consisting 1:1 mole ratios of DMPA and DMPC-$d_{54}$ display no lateral segregation of components at either pH 7.0 or 4.0 in the presence of the sodium cation. Although calcium clearly induces a lateral phase separation of the lipid components in the DMPA + DMPC-$d_{54}$ system at pH 7.5 (4), no distinct lateral segregation of the lipid components is observed in this binary lipid mixture at

pH 4.0. Domain formation, consisting of regions rich in DMPA and DMPC-$d_{54}$, respectively, is suggested, however, for the calcium binary lipid mixture at pH 4.0 by the different phase transition properties for the separate DMPA and DMPC-$d_{54}$ species.

The interactions of these lipid systems with ferricytochrome *c* is manifest in the disorder induced by the protein-lipid complexes. Ferricytochrome *c* forms complexes with sodium DMPA bilayers at both pH 7.0 and 4.0 which exhibit considerably disordered structures, especially at temperatures above 40°C. The lipid structure for these sodium DMPA-ferricytochrome *c* complexes is more disrupted than the similar calcium DMPA-ferricytochrome assemblies. Calcium in the DMPA-ferricytochrome *c* complex coordinates the head group to form a stable bilayer structure that is not easily perturbed by the protein, even at higher temperatures where the protein denatures. Earlier studies of calcium complexes of 1:1 mixtures of DMPA and DMPC-$d_{54}$ lipids indicated lateral phase separation of the two lipids at pH 7.5 (4). Evidence of domain structures being induced by ferricytochrome *c* in a ternary lipid-protein complex (protein + DMPA + DMPC-$d_{54}$) is suggested for the sodium cation at pH 7.0. However, the ternary mixtures lipid system with calcium at both pH 4.0 and 7.0 do not undergo lateral separation of their lipid components. These results emphasize the considerable effect small concentrations of ferricytochrome *c* have on the order of lipid bilayer assemblies containing anionic constituents.

The authors wish to acknowledge invaluable discussions with Drs. Ralph Adams, Neil Lewis, and Mark Devlin concerning various aspects of this work. Mr. John Powell of the National Institutes of Health Division of Computer Research and Technology was of considerable help in the data analysis and graphical renditions.

*Received for publication 7 November 1990 and in final form 24 January 1991.*

## REFERENCES

1. Van den Bosch, H. 1974. Phosphoglyceride metabolism. *Annu. Rev. Biochem.* 43:243–277.
2. Berridge, M. J. 1984. Inositol triphosphate and diacylglycerol as second messages. *Biochem. J.* 220:345–360.
3. Smaal, E. B., J. G. Mandersloot, R. A. Demel, B. de Kruijff, and J. de Gier. 1987. Consequences of the interaction of calcium with dioleoylphosphatidate-containing model membranes: calcium-membrane and membrane-membrane interactions. *Biochem. Biophys. Acta.* 897:180–190.
4. Kouaouci, R., J. R. Silvius, I. Graham, and M. Pézolet. 1985. Calcium-induced lateral phase separations in phosphatidylcholine-phosphatidic acid mixtures. *Biochemistry.* 24:7132–7140.
5. Koppenol, W. H., and E. Margoliash. 1982. The asymmetric distribution of charges on the surface of horse cytochrome *c*: functional implications. *J. Biol. Chem.* 257:4426–4437.
6. Nicholls, P. 1974. Cytochrome *c* binding to enzymes and membranes. *Biochim. Biophys. Acta.* 346:261–310.
7. Quinn, P. J., and R. M. C. Dawson. 1969. Interactions of cytochrome *c* and [$^{14}$C]carboxymethylated cytochrome *c* with monolayers of phosphatidylcholine, phosphatidic acid and cardiolipin. *Biochem. J.* 115:65–75.
8. Kimelberg, H. K., and C. P. Lee. 1970. Interactions of cytochrome *c* with phospholipid membranes: II. Reactivity of cytochrome *c* bound to phospholipid liquid crystals. *J. Membr. Biol.* 2:252–262.
9. Brown, L. R., and K. Wüthrich. 1977. NMR and ESR studies of the interactions of cytochrome *c* with mixed cardiolipin-phosphatidylcholine vesicles. *Biochim. Biophys. Acta.* 468:389–395.
10. Birrel, G. B., and O. H. Griffith. 1976. Cytochrome *c* induced lateral phase separation in a diphosphatidylglycerol-steroid spin-label model membrane. *Biochemistry.* 15:2925–2929.
11. Vincent, J. S., H. Kon, and I. W. Levin. 1987. Low-temperature electron paramagnetic resonance study of the ferricytochrome *c*-cardiolipin complex. *Biochemistry.* 26:2312–2314.
12. Vincent, J. S., and I. W. Levin. 1986. Interaction of ferricytochrome *c* with cardiolipin multilayers: a resonance Raman study. *J. Am. Chem. Soc.* 108:3551–3554.
13. Dickerson, R. E., T. Takano, D. Eisenberg, O. B. Kallai, L. Samson, A. Cooper, and E. Margoliash. 1971. Ferricytochrome *c*: I. General features of the horse and bonito proteins at 2.8 A resolution. *J. Biol. Chem.* 246:1511–1535.
14. Vincent, J. S., and I. W. Levin. 1988. Interaction of ferricytochrome *c* with zwitterionic phospholipid bilayers: a Raman spectroscopic study. *Biochemistry.* 27:3438–3446.
15. Harlos, K., H. Elbl, I. Pascher, and S. Sundell. 1984. Conformation and packing properties of phosphatidic acid: the crystal structure of monosodium dimyristoylphosphatidate. *Chem. Phys. Lipids.* 34:115–126.
16. Papahadjopoulos, D., W. J. Vail, W. A. Pangborn, and G. Poste. 1976. Studies on membrane fusion: induction of fusion in pure phospholipid membranes by calcium ions and other divalent metals. *Biochim. Biophys. Acta.* 448:265–283.
17. Liao, M. J., and J. H. Prestegard. 1981. Structural properties of a $Ca^{2+}$-phosphatidic acid complex, small angle x-ray and calorimetric results. *Biochim. Biophys. Acta.* 645:149–156.
18. Eibl, H., and P. Woolley. 1979. Electrostatic interactions at charged lipid membranes. Hydrogen bonds in lipid membranes surfaces. *Biophys. Chem.* 10:261–271.
19. Eibl, H., and A. Blume. 1979. The influence of charge on phosphatidic acid bilayer membranes. *Biochim. Biophys. Acta.* 553:476–488.
20. Blume, A., and H. Eibl. 1979. The influence of charge on bilayer membranes: calorimetric investigations of phosphatidic acid bilayers. *Biochim. Biophys. Acta.* 558:13–21.
21. Levin, I. W. 1984. Vibrational Spectroscopy of Membrane Assemblies, Advances in Raman and Infrared Spectroscopy. R. J. H. Clark, and R. E. Hester, editors. Heyden & Son, Ltd., London. 11:1–48.
22. Levin, I. W. 1985. Structural and Dynamical Properties of Model and Intact Membrane Assemblies by Vibrational Spectroscopy, Chemical, Biological and Industrial Applications of Infrared Spectroscopy. J. R. Durig, editors. John Wiley and Sons, New York. 173–197.

23. Gaber, B. P., and W. L. Peticolas. 1977. On the quantitative interpretation of biomembrane structure by Raman spectroscopy. *Biochim. Biophys. Acta.* 465:260–274.

24. Spiker, R. C., and I. W. Levin. 1976. Effect of bilayer curvature on vibrational Raman spectroscopic behavior of phospholipid-water assemblies. *Biochim. Biophys. Acta.* 455:560–575.

25. Hill, I. R., and I. W. Levin. 1979. Vibrational spectra and carbon-hydrogen stretching mode assignments for a series of *n*-alkyl carboxylic acids. *J. Chem. Phys.* 70:842–851.

26. Huang, C., J. R. Lapides, and I. W. Levin. 1982. Phase-transition behavior of saturated, symmetric chain phospholipid bilayer dispersions determined by Raman spectroscopy: correlation between spectral and thermodynamic parameters. *J. Am. Chem. Soc.* 104:5926–5930.

27. Mendelsohn, R., and T. Taraschi. 1978. Deuterated phospholipids as Raman spectroscopic probes of membrane structure: dipalmitoylphosphatidylcholine-dipalmitoylphosphatidylethanolamine. *Biochemistry.* 17:3944–3949.

28. Mendelsohn, R., and J. Maisano. 1978. Use of deuterated phospholipids in Raman spectroscopic studies of membrane structure: I. Multilayers of dimyristoylphosphatidylcholine (and its $d_{54}$ derivative) with distearoylphosphatidylcholine. *Biochim. Biophys. Acta.* 506:192–201.

29. Mendelsohn, R., and C. C. Koch. 1980. Deuterated phospholipids as Raman spectroscopic probes of membrane structure: phase diagrams for dipalmitoylphosphatidylcholine (and its $d_{54}$ derivative)-dipalmitoylphosphatidylethanolamine system. *Biochem. Biophys. Acta.* 598:260–271.

30. Bryant, G. J., F. Lavialle, and I. W. Levin. 1982. Effects of membrane bilayer reorganizations on the 2103 $cm^{-1}$ Raman spectral C-D stretching mode linewidths in dimyristoyl phosphatidylcholine-$d_{54}$ (DMPC-$d_{54}$) liposomes. *J. Raman Spectrosc.* 12: 118–121.

31. Devlin, M. T., and I. W. Levin. 1990. Acyl chain packing properties of deuterated lipid bilayer dispersions: vibrational Raman spectral parameters. *J. Raman Spectrosc.* 21:441–452.

32. Brautigan, D. L., S. Ferguson-Miller, and E. Margoliash. 1978. Mitochondrial cytochrome *c*: preparation and activity of the native and chemically modified cytochromes *c*. *Methods Enzymol.* 53:128–148.

33. Kirchhoff, W. H., and I. W. Levin. 1987. Description of the thermotropic behavior of membrane bilayers in terms of Raman spectral parameters: a two-state model. *J. Res. Natl. Bureau Standards.* 92:113–128.

34. Mushayakarara, E., N. Albon, and I. W. Levin. 1982. Effects of water on the molecular structure of a phosphatidylcholine hydrate. *Biochim. Biophys. Acta.* 686:153–159.

35. Bush, S. F., R. G. Adams, and I. W. Levin. 1980. Structural reorganizations in lipid bilayer systems: effect of hydration and sterol addition on Raman spectra of dipalmitoylphosphatidylcholine multilayers. *Biochemistry.* 19:4429–4436.

36. Hauser, H., and R. M. C. Dawson. 1967. The binding of calcium at lipid-water interfaces. *Eur. J. Biochem.* 1:61–69.

37. Trauble, H., and H. Eibl. 1974. Electrostatic effects on the lipid phase transitions: membrane structure and ionic environment. *Proc. Natl. Acad. Sci. USA.* 71:214–219.